

# Sub-kHz-linewidth VECSELs for cold atom experiments

PAULO HISAO MORIYA,<sup>1,\*</sup>  YESHPAL SINGH,<sup>2</sup> KAI BONGS,<sup>2</sup> AND JENNIFER E. HASTIE<sup>1</sup>

<sup>1</sup>*Institute of Photonics, Department of Physics, SUPA, University of Strathclyde, Technology and Innovation Centre, 99 George Street, Glasgow G1 1RD, UK*

<sup>2</sup>*School of Physics and Astronomy, University of Birmingham, B15 2TT Birmingham, UK*

\*[paulo.moriya@strath.ac.uk](mailto:paulo.moriya@strath.ac.uk)

**Abstract:** We report and characterize sub-kHz linewidth operation of an AlGaInP-based VECSEL system suitable for addressing the narrow cooling transition of neutral strontium atoms at 689 nm. When frequency-stabilized to a standard air-spaced Fabry-Perot cavity (finesse 1000) via the Pound-Drever-Hall (PDH) technique, it delivers output power >150 mW in a circularly-symmetric single transverse mode with low frequency and intensity noise. The optical field was reconstructed from the frequency noise error signal via autocorrelation and the Wiener-Khinchine theorem, leading to an estimated linewidth of  $(125 \pm 2)$  Hz. Optical beat note measurements were performed against a commercial locked laser system and a second, almost identical, VECSEL system resulting in linewidths of 200 Hz and 160 Hz FWHM, respectively. To the best of our knowledge, this is the first demonstration of a VECSEL compatible with the narrowest of lines (few hundred Hz) used for cooling and trapping atoms and ions.

Published by The Optical Society under the terms of the [Creative Commons Attribution 4.0 License](https://creativecommons.org/licenses/by/4.0/). Further distribution of this work must maintain attribution to the author(s) and the published article's title, journal citation, and DOI.

## 1. Introduction

Stable, high power, narrow linewidth, and tunable laser sources are crucial for a wide range of applications in several scientific [1–3] and industrial fields [4–6]. In particular, they are required for the development of quantum technologies based on cold atoms with transitions at optical frequencies [7]. The lasers used in many of the current systems are based on extended cavity diode lasers (ECDLs). These lasers require stabilization, if no atomic reference is available at room temperature [8], to sophisticated and expensive reference cavities, with ultra-high stability and finesse, to reduce the free-running linewidth from hundreds of kHz to Hz [9]. In this case, a narrow full-width at half maximum (FWHM) linewidth may still not be indicative of sufficient spectral purity, given the broad phase noise ‘pedestal’ typical of high gain, edge-emitting semiconductor lasers, which have significant fast frequency noise [10]. Further, depending on the required emission wavelength, these systems often do not provide sufficient optical power. As a result, amplifiers [11], or injection lock schemes [12,13], need to be employed, particularly if a nonlinear frequency conversion stage is also to be implemented. To improve the wavelength coverage of the visible part of the electromagnetic spectrum, due to the emergence of exotic atomic species with narrow and clock transitions, different laser technologies have been explored but present similar limitations in power or on the required stabilization system [14,15].

In this context VECSELs [16], also known as semiconductor disk lasers (SDLs), have demonstrated great potential due to their spectral flexibility (from UV to IR), power scaling, high beam quality and brightness, and suitability for low noise single frequency operation [17,18]. The vertical format allows the quantum wells to be positioned with nm-scale accuracy with respect to the anti-nodes of the optical field (known as resonant periodic gain [19]), such that hole-burning is avoided and ring-cavity oscillation is not required for stable single frequency operation [20].

Potential for miniaturization is another attractive feature as these lasers are compact, with any frequency conversion and filtering performed intracavity, and the low-divergence circularly-symmetric, single transverse mode output beam enables fiber-coupling with very low loss. Indeed, while these are typically optically-pumped lasers (electrically-injected VECSELs are, to date, only available within a limited wavelength range; see e.g [21].), the addition of a compact diode pump unit can be offset against the external amplifiers, frequency-conversion stages and associated beam-shaping optics required to approach the same performance with an ECDL, even before the addition of frequency stabilization instrumentation. The combination of high output power, very high finesse resonators, and very low spontaneous emission factor for these lasers means that the fundamental limit to the laser linewidth, known as the Schawlow-Townes-Henry limit [22,23], is as low as mHz for VECSELs, compared with a few tens of kHz for a typical ECDL [24]. Further, due to the high ratio of photon lifetime ( $>30$  ns) to gain lifetime (few ns), relaxation oscillations are completely damped, in contrast to both solid-state lasers ( $> \mu$ s gain lifetime) and ECDLs (typically  $<$  ns photon lifetime). Low intensity and frequency noise operation of VECSELs, down to a few kHz, have been achieved over timescales of the order of 1s [17,18,25], but sub-kHz or lower linewidths, such as those required for narrow atom cooling and clock transitions, have yet to be reported.

In this paper we report frequency stabilization of an AlGaInP-based VECSEL locked, via the Pound-Drever-Hall (PDH) technique [26,27], to a standard commercial air-spaced Fabry-Perot cavity, achieving  $<200$  Hz linewidth with output powers  $>150$  mW. The frequency noise was first characterized by calculating the RMS noise and power spectral density (PSD) as a function of Fourier frequency from the residual error signal of the locking system. From the PSD, the spectral shape of the optical field can be reconstructed via auto-correlation and the Wiener-Khintchine theorem so that the linewidth can be estimated [28]. This result is validated by performing optical beat note measurements against both another VECSEL system locked to the same reference cavity via the side-of-fringe technique [17], and a commercial ECDL system locked to an ultra-stable cavity stabilized in a vacuum chamber. The emission wavelength can be tuned from 685 to 693 nm, suitable for use as part of Strontium cold atoms experiments; specifically, for targeting the second-stage cooling transition used for Strontium magneto-optical traps: 689.4488968 nm (transition linewidth = 7.6 kHz) [29–31].

## 2. VECSEL multi-quantum well gain structure and laser performance

The VECSEL gain structure used to achieve narrow linewidth operation is similar to those reported previously by our group [32,33]. The first component of the structure, grown on a GaAs substrate, is a semiconductor mirror (distributed Bragg reflector) composed of AlGaAs/AlAs layers with high-reflectivity at 690 nm. The active region consists of 10 pairs of compressively-strained GaInP quantum wells (QWs) positioned at the optical field anti-nodes for resonant periodic gain [see Fig. 1(a)], with lattice-matched AlGaInP barriers and tensile-strained compensation layers at the field nodes (see e.g [16].). The structure is designed to be optically-pumped at green wavelengths with emission wavelength  $\sim 689$  nm.

A  $4 \times 4$  mm<sup>2</sup> chip was cleaved, capillary bonded with deionized water to a 4-mm-diameter, 500- $\mu$ m-thick diamond heat spreader, before being clamped to a brass mount kept at 18°C via thermo-electric cooling. The 10-cm-long laser cavity is completed by a 2% transmission plano-concave output coupler (OC) with minimized bulk ( $\varnothing = 6$  mm, thickness = 3 mm, mass = 2 g and RoC = -100 mm), mounted via epoxy on a ring actuator piezoelectric transducer (PZT; P-010.00H from Physik Instrumente) for active frequency stabilization. The PZT was in turn secured with epoxy to a commercial mirror mount. Intracavity, a 6-mm-thick quartz plate is placed at Brewster's angle to be used as a birefringent filter (BRF) for wavelength tuning, [see top left corner of Fig. 1(b)]. In order to reduce the impact of any mechanical, acoustic and thermal

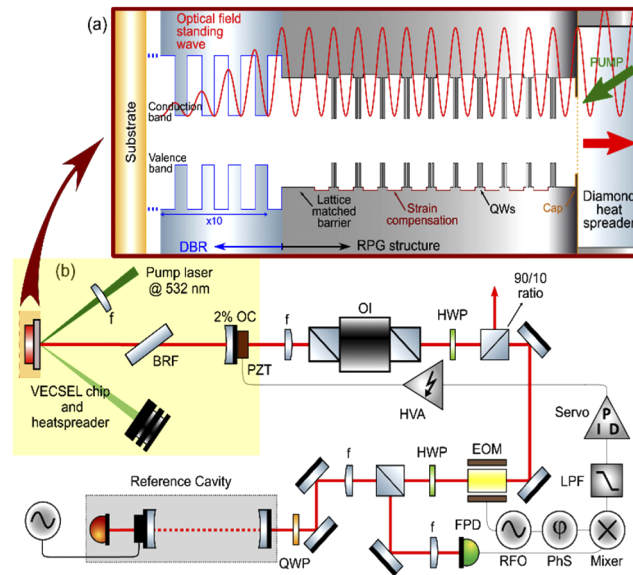


**Fig. 1.** (a) Schematic of the VECSEL gain structure, and (b) laser cavity and frequency stabilization system. Highlighted at the top left corner is the two-mirror laser cavity with a total length of 10 cm, formed by the semiconductor gain mirror and a 2% transmission, plano-concave output coupler (OC). The laser linewidth is reduced by implementing active frequency stabilization via the Pound-Drever-Hall (PDH) technique. A fraction of the output laser beam (~10%) is picked off by a beam splitter, phase-modulated by an electro-optic modulator (EOM), and coupled to a moderately-high-finesse reference cavity (confocal Fabry-Perot, finesse = 1000 and free spectral range = 300 MHz). The reflected spectrum is captured by a fast-photodetector (FPD) to create an error signal which is sent back to the laser cavity via a piezo electric transducer (PZT) on which the OC is mounted. DBR: distributed Bragg reflector; RPG: resonant periodic gain; QW: quantum wells; BRF: birefringent filter; HWP: half-wave plate; QWP: quarter-wave plate; OI: optical isolator; PhS: phase shifter; RFO: radio frequency oscillator; LPF: low-pass filter; HVA: high-voltage amplifier.

fluctuations in the laser performance, the optical system is built inside an optical enclosure on a breadboard with passive vibration isolation on a standard floating optical table.

Laser oscillation is achieved by optically-pumping the gain structure with a compact, commercial semiconductor laser system at 532 nm (with power up to 5 W) in a 90- $\mu\text{m}$ -diameter focal spot. The VECSEL emission wavelength is tuned to the correct value with sub-pm precision by using both the intracavity BRF and small changes to the sample temperature [33]. The former provides coarse tunability in steps of 200 pm when rotated in its axis, related to the free spectral range of the heat spreader; the latter allows fine, continuous tuning of the wavelength within the free spectral range of the BRF (30 pm). Finally, single frequency operation is achieved by careful optimization of the cavity for single mode oscillation. Figure 2(a) and Fig. 2(b) summarize our red VECSEL system performance.

As expected the VECSEL system delivers high brightness in multi-mode operation, reaching 0.5 W (slope efficiency of 19.6% and conversion efficiency of 14%) when the intracavity filter is absent. Tunable single frequency operation with high output power is achieved by introducing the BRF, carefully aligning the laser cavity and optimizing its length. In common with other single-mode VECSELs (see e.g [18].), the output beam quality is excellent, suitable for efficient fiber-coupling. In this regime, slope efficiency of 15.5% with threshold of 1.0 W is measured, with thermal rollover above 2.7 W of absorbed optical pump power. For the measurements

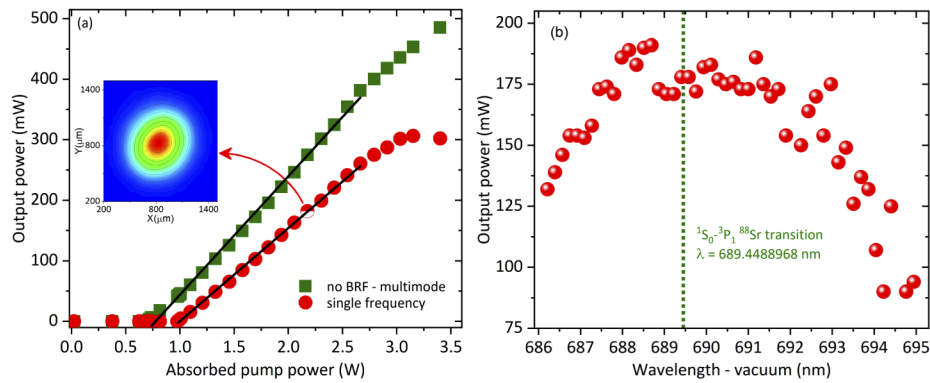


**Fig. 2.** (a) VECSEL system power transfer measurements with (single frequency, red circles) and without (green squares) an intracavity birefringent filter (BRF). *Inset:* VECSEL beam profile for single frequency operation at 170 mW output power (2.3 W pump), measured 10 cm after the output coupler. (b) Output wavelength tunability curve for 2.3 W pump power, achieved by rotating the BRF in its axis. The emission can be tuned between 686 and 695 nm. Green dotted line (vertical): wavelength of the narrow second cooling transition of  $^{88}\text{Sr}$  ( $^1\text{S}_0 - ^3\text{P}_1$ ).

presented hereafter, the pump power is reduced to 2.3 W so that the VECSEL sample temperature can be used to tune the emission wavelength without compromising the performance of the temperature controller and thermo-electric cooler via overloading ( $I_{\text{max}} = 2 \text{ A}$ ,  $P_{\text{max}} = 12 \text{ W}$ ). At this optical pump power, the emission wavelength can be tuned with output power greater than 90 mW between 686 and 695 nm by rotating the BRF. At the wavelength required for second stage cooling of neutral strontium, 689.4 nm, powers up to 170 mW are measured.

On the same breadboard, the frequency stabilization system for the Pound-Drever-Hall technique is assembled [see Fig. 1(b)] to suppress external noise influences and reduce the laser linewidth towards the second Strontium cooling transition requirement. First, the output laser beam is collimated to a diameter of 1.5 mm before passing through an optical isolator with manufacturer-specified isolation of  $\sim 30 \text{ dB}$  at 689 nm. A half-wave plate and polarizing beam-splitter cube are used to pick off a small fraction of the power ( $\sim 10\%$ ) for the stabilization set-up such that the majority of the power ( $> 120 \text{ mW}$ ) is available to send directly to the cold atoms experiment. The pick-off beam is phase modulated (frequency modulation of 74 MHz and RF power  $< 20 \text{ dBm}$ ) by an electro-optical modulator (EOM) and coupled to a moderately-high-finesse, air-spaced, confocal Fabry-Perot cavity (finesse = 1000, free spectral range = 300 MHz). The transmitted spectrum is used to monitor the laser performance and the reflection is captured by a fast-photodetector to create an error signal that is delivered to the PZT, on which the laser OC is mounted, via a servo controller and a high voltage amplifier, closing the feedback loop. To characterize the correction bandwidth we applied a sinusoidal signal to the PZT and measured the frequency-dependent output to produce a transfer function [34]. The combination of a PZT with a low size and weight output coupler results in a high correction bandwidth of 30 kHz with a total excursion of 5  $\mu\text{m}$ .

### 3. Frequency and intensity noise analysis

When the PDH frequency stabilization is switched on (frequency discriminator = 210 V/MHz), the laser remains locked to the reference cavity for several 10s of minutes limited by thermal drifts of the laser and reference cavity (estimated to be  $< 10 \text{ kHz/min}$ , limited by the resolution of our wavemeter), and residual mechanical noise. The servo controller gain and local oscillator

amplitude modulation are kept at minimum values so that high frequency noise presents a negligible contribution to the laser linewidth [35].

The VECSEL frequency noise performance and linewidth is first characterized by recording the residual (AC) error signal from the servo controller over a range of acquisition times, from 10  $\mu$ s to 1000 s, limited by the detector speed and oscilloscope memory respectively. The RMS noise did not vary significantly over this range of acquisition times, remaining around  $(330 \pm 30)$  Hz [see inset Fig. 4(b)]. The power spectral density (PSD),  $S_v(f)$  (see Fig. 3), which was calculated via the method presented in [36], presents a noise floor reduction  $>50$  dB at a few Hz when the active stabilization is switched on. The majority of the frequency noise in the stabilized PSD (75%) is concentrated at frequencies above 100 kHz. In this region, peaks are related to noise originating in the feedback loop and pump laser intensity noise. The noise band below 1 kHz contributes another 5% of pure mechanical and thermal noise, with peaks at 50 and 150 Hz related to the mains electricity frequency and harmonics. Finally, the 1-100 kHz band, which contributes 20%, presents a broad resonance at 7 kHz which represent mechanical modes of the VECSEL, BRF, and output coupler mounts. It also includes noise transferred to the VECSEL by the pump laser system that is not filtered out by the external laser cavity (acting as a low-pass filter with finesse = 300 and cutoff-frequency = 2.4 MHz); this contributes to the noise floor and leads to peaks around and above 20 kHz. Figure 3 also shows the  $\beta$ -separation line, defined as  $S_\beta(f) = 8(\ln 2)f/\pi^2$  [28], where  $f$  is Fourier frequency, which divides the frequency noise PSD graph into two regions: the first, delimited by  $S_\beta(f) < S_v(f)$  directly affects the central part (Gaussian) of the laser line shape resulting in changes to the linewidth; the second, defined by  $S_\beta(f) > S_v(f)$ , represents frequency fluctuations too fast to affect the laser linewidth, contributing only to the wings of the line shape (Lorentzian). The linewidth of the laser can thus be estimated via  $\delta\Delta\nu_{\text{FWHM}} \cong \sqrt{8 \ln 2 A}$ , where  $A$  is the area under the frequency noise power spectral density curve for frequencies exceeding the separation line. We thus estimate a linewidth of 150 kHz for the free-running laser. For the locked laser, however, sufficient acquisition time must be used to avoid under-sampling at low frequencies, depending on where the  $\beta$ -separation line divides the spectrum. Figure 4(a) shows the calculated power spectral density at low frequencies for an acquisition time of 100 s. This results in an estimated linewidth of 112 Hz for the locked laser.

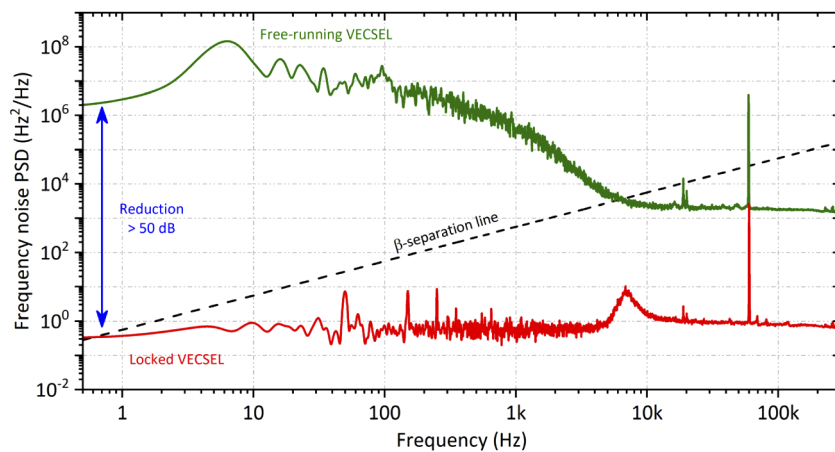


**Fig. 3.** Calculated power spectral density (PSD) from the residual error signal recorded over 2s. Noise reduction of  $>50$  dB is observed when active frequency stabilization is switched on.

Alternatively, the laser linewidth can be estimated by reconstructing the shape of the optical field via auto-correlation and the Wiener-Khintchine theorem. This technique is used to estimate

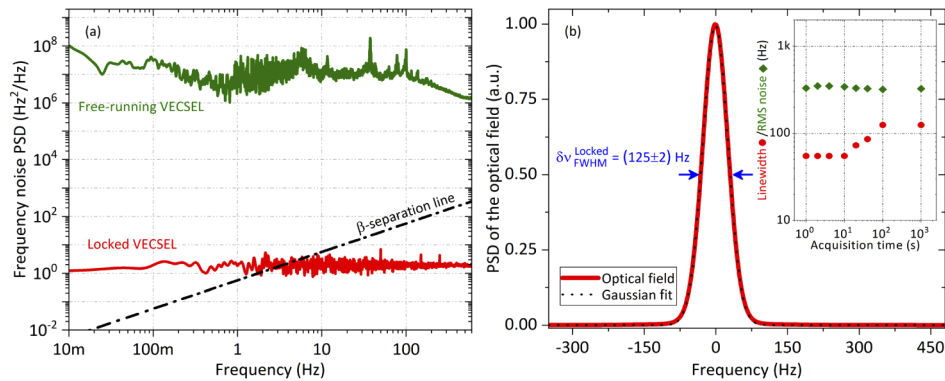


**Fig. 4.** Linewidth estimate for the locked VECSEL system. (a) Frequency noise power spectral density (PSD) calculated for an acquisition time of 100 s. (b) Power spectral density of the optical field reconstructed via autocorrelation and the Wiener-Khinchine theorem from the spectrum for the locked laser presented in (a). A linewidth of  $(125 \pm 2)$  Hz was estimated from the Gaussian fit. Inset: RMS noise for a range of acquisition times together with the linewidths estimated via Gaussian fits of the optical fields reconstructed via autocorrelation and the Wiener-Khinchine theorem.

laser linewidth relative to a suitable reference when no other laser is available or where a self-heterodyne measurement is impractical [28,37,38]. A linewidth of  $(125 \pm 2)$  Hz is estimated [see Fig. 4(b)] for the central (or Gaussian) part of the emission spectrum for acquisition times of 100 s and up to 1000 s, limited by the memory of our oscilloscope (see inset).

Figure 5 shows the measured relative intensity noise (RIN) of the VECSEL and pump system. The pump laser curve presents peaks only at frequencies above 15 kHz. These peaks, which are transferred from the pump to the free running VECSEL, and also contribute to the frequency noise [39], are removed with the active frequency stabilization. The RIN curve for the VECSEL system shows that the majority of the noise peaks are below 1 kHz (dominant peak around 200 Hz), which highlights the mechanical and thermal nature of the intensity noise in our system. Intensity noise in this region can be further reduced by improving the overall laser cavity stability, which is currently based on standard commercial, free-space optical mounts. The measured VECSEL RIN reaches values as low as -153 dBc/Hz, approaching the shot noise limit (-160 dBc/Hz).

In order to validate the linewidth and stability results presented above, optical beat note measurements were performed. Initial measurements were performed using a commercial ECDL system with tapered amplifier, locked to an ultra-stable and ultra-high-finesse cavity 102 MHz away from the VECSEL emission. The finesse achieved with this cavity was 300k (FSR 1.5 GHz), and it was kept in a temperature-stabilized vacuum chamber to reduce thermal and mechanical noise, achieving a linewidth of 1 Hz (FWHM). Up to 160 mW output power is available before fiber-coupling. The beat note peak with this stabilized output and the VECSEL was recorded in a spectrum analyzer, resulting in a FWHM of  $(200 \pm 2)$  Hz [41] [see Fig. 6(b)]. Here, the lasers were located in different laboratories with the ECDL coupled via optical fiber, which is likely to have led to broadening of the beat note from additional mechanical and thermal noise, unrelated to the laser performance. For a more complete performance analysis over longer acquisition times, a second VECSEL system (with an almost identical design to that presented above) was built and locked to the same reference cavity as the first VECSEL via the side-of-fringe technique. The lasers were locked to different TEM modes of the cavity (00 and 01), separated by 140 MHz. The second VECSEL, when compared to the one locked via PDH, presents higher intensity and amplitude noise but similar frequency noise, with a slightly broader linewidth of

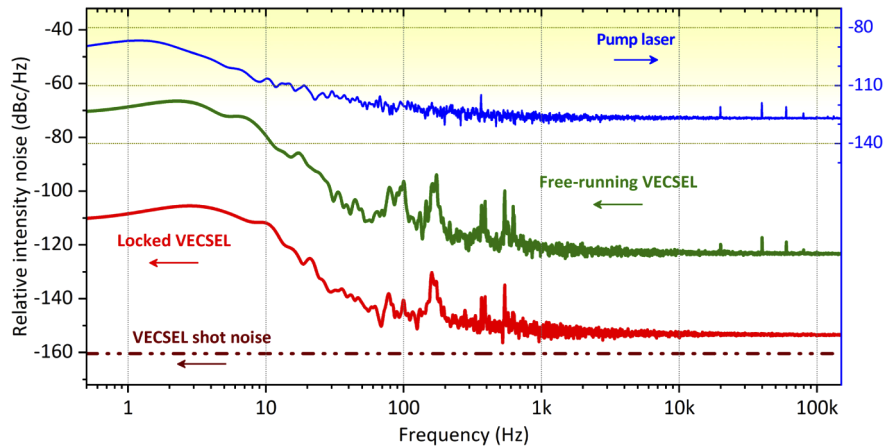


**Fig. 5.** Relative intensity noise graphs for the pump laser; the free-running VECSEL; and for the locked VECSEL system, measured with a detector bandwidth of 150 kHz. The most dominant peaks ( $f < 1$  kHz) are related to thermal and mechanical noise. Pump intensity noise ( $f > 20$  kHz) is transmitted to the free-running VECSEL output.

( $155 \pm 2$ ) Hz for acquisition time of 100 s, calculated via the same Wiener-Khinchine method. As expected, its stability performance depends strongly on environmental noise, being limited to acquisition ranges  $< 500$  s. The overlapped beams were captured over a given acquisition time by a fast photodetector, and the generated RF signal was simultaneously measured by an electronic spectrum analyzer and an oscilloscope. Figure 6(a) shows the beat note peak at 140 MHz with a full-width at half-maximum ( $-3$  dB) of ( $160 \pm 5$ ) Hz (RBW = 10 Hz, sweep time 10 s, 100 measurements averaged); very close to the expected limit set by the laser with the broadest linewidth. Some side peaks, suppressed by a factor of  $> 25$  dB, are present around the beat note and are the result of a residual low frequency modulation originating in the servo controller electronics used for frequency-stabilizing the breadboard VECSEL system. This beat

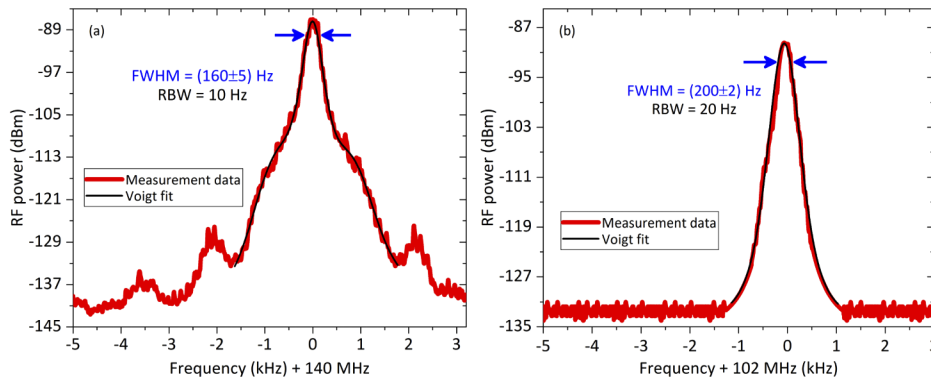


**Fig. 6.** Optical beat note measurement performed against (a) another VECSEL system locked to a different mode of the same reference cavity via the side-of-fringe technique (sweep time: 10 s; 100 measurements averaged), and (b) a commercial system locked to an ultra-stable, ultra-high-finesse cavity via the Pound-Drever-Hall technique (sweep time: 0.5 s; 10 measurements averaged). Linewidths, obtained via Voigt fits to the data [40], are ( $160 \pm 5$ ) Hz and ( $200 \pm 2$ ) Hz, respectively, at  $-3$  dB (FWHM). RBW: resolution bandwidth of the spectrum analyzer used in each case.

note measurement again supports the sub-kHz performance; however, it should be noted that the common reference cavity may result in frequency and phase noise correlations and common mode rejection which can lead to an underestimate of the linewidths of the lasers. Nevertheless, the PSD analysis and the upper limit for the beat note with the ultra-stable ECDL system provide evidence that this is not the case here.

#### 4. Discussion

The 125-Hz-linewidth performance presented here is, to the best of our knowledge, the first demonstration of a VECSEL system compatible with the narrowest of transition lines used for trapping atoms and ions, representing at least an order of magnitude improvement over linewidths previously reported for such laser systems [42,43]. When compared to other actively-frequency-stabilized laser technologies, such as diode and fiber lasers, the frequency noise spectrum of the VECSEL system presented here is also composed mainly of white and flicker noise but at reduced levels with lower contribution of the mechanical instabilities and intensity noise components typical of such systems [39], notwithstanding our choice of an air-spaced Fabry-Perot cavity as a frequency reference. In fact, current research and development of ECDL-based systems at this wavelength is focused on increasing the passive-stability of the mounts [44], the reduction of the overall size and number of components of the system [45], and locking to references with higher stability such as frequency combs [46] and state-of-art ultra-stable cavities [47]. Indeed, the capability to achieve such results with a reference of only moderate finesse is important to reduce costs and improve the portability of ultra-low noise, ultra-stable laser systems and is enabled by the intrinsic low noise and high brightness of the VECSEL technology. While this system is currently pumped at green wavelengths, the gain structure can be adjusted for pumping with high power blue diodes [48,49], now widely available at low cost, with the added advantage of pump intensity stabilization via modulation of the current (VECSELS, as broadband, planar absorbers, are insensitive to the wavelength, linewidth, frequency noise, or spatial brightness of the pump). Further, we see no reason why this performance could not be readily translated to any other wavelength within the broad range available to VECSELS systems, i.e. from the ultraviolet to the mid-infrared via a combination of semiconductor bandgap engineering and second harmonic generation achieved within the same, stabilized cavity (see e.g [33]). The fundamental, or Schawlow-Townes-Henry, limit for an AlGaInP VECSEL is expected to be  $10^{-4}$  Hz (calculated following [50]), orders of magnitude lower than any other semiconductor laser technology. Finally, the high brightness fundamental emission at 689 nm represents a significant gain in optical power in comparison to ECDL systems commonly used in Strontium cold atoms experiments (see e.g [46,51]), which require external amplification systems to achieve comparable power.

#### 5. Conclusions

We have demonstrated and characterized sub-kHz-linewidth, single-frequency operation of a VECSEL system locked to a commercial air-spaced Fabry-Perot cavity via the Pound-Drever-Hall technique. The emission wavelength is centered at 689 nm with multi-100 mW output power. The narrow laser linewidth was first estimated by calculating the geometrical area of the frequency noise power spectral density with high modulation (or above the  $\beta$ -separation line) [28]. The second method used the autocorrelation function and the Wiener-Khinchine theorem to reconstruct the central part (Gaussian) of the shape of the optical field. These methods resulted in estimated linewidths of 112 and  $(125 \pm 2)$  Hz, respectively. Finally, optical beat note measurements against a second VECSEL system locked to a different mode of the same reference cavity, and a commercial tapered-amplified ECDL system locked to an ultra-stable, ultra-high-finesse cavity were performed, resulting in beat note linewidths of  $(160 \pm 5)$  Hz and  $(200 \pm 2)$  Hz, respectively. A full frequency and intensity noise characterization was also presented



highlighting the influence of pure and thermally-induced mechanical noises in our setup. As this laser was built using standard moveable air-spaced optical mounts, these noise contributions can be significantly reduced via engineering a custom, rigid laser enclosure. Thus the free running and locked laser linewidth can be pushed further towards the Schawlow-Townes-Henry limit, predicted to be  $\sim 1$  mHz for this laser technology. With the performance presented above, the VECSEL system can be used as part of a neutral Strontium magneto-optical trap setup targeting the narrow second cooling transition, offering a significant brightness improvement over the current ECDL lasers at these wavelengths, and enabling the development of portable optical clocks for quantum technologies.

## Funding

Engineering and Physical Sciences Research Council (EP/I022791/1, EP/M013294/1).

## Acknowledgments

The laser gain structures were grown by Dr Andrey Krysa at the EPSRC National Centre for III-V Technologies. The laser enclosure for the second VECSEL, used in the beat note measurement system, was supplied by Dr Peter Schlosser of the Fraunhofer Centre for Applied Photonics. Data related to this publication have been made available at the University of Strathclyde data repository [52].

## Disclosures

The authors declare no conflicts of interest.

## References

1. M. Takamoto, F. L. Hong, R. Higashi, and H. Katori, "An optical lattice clock," *Nature* **435**(7040), 321–324 (2005).
2. B. S. Sheard, G. Heinzel, K. Danzmann, D. A. Shaddock, W. M. Klipstein, and W. M. Folkner, "Intersatellite laser ranging instrument for the GRACE follow-on mission," *J Geod* **86**(12), 1083–1095 (2012).
3. S. Gundavarapu, G. M. Brodnik, M. Puckett, T. Huffman, D. Bose, R. Behunin, J. F. Wu, T. Q. Qiu, C. Pinho, N. Chauhan, J. Nohava, P. T. Rakich, K. D. Nelson, M. Salit, and D. J. Blumenthal, "Sub-hertz fundamental linewidth photonic integrated Brillouin laser," *Nat. Photonics* **13**(1), 60–67 (2019).
4. E. Nieves, N. Xi, X. Li, C. Martinez, and G. Zhang, "Laser beam multi-position alignment approach for an automated industrial robot calibration," in *The 4th Annual IEEE International Conference on Cyber Technology in Automation, Control and Intelligent*, 2014), 359–364.
5. X. D. Gao, D. Y. You, and S. Katayama, "The high frequency characteristics of laser reflection and visible light during solid state disk laser welding," *Laser Phys. Lett.* **12**(2015).
6. S. Rerucha, A. Yacoot, T. M. Pham, M. Cizek, V. Hucl, J. Lazar, and O. Cip, "Laser source for dimensional metrology: investigation of an iodine stabilized system based on narrow linewidth 633 nm DBR diode," *Meas. Sci. Technol.* **28**(4), 045204 (2017).
7. L. Fallani and A. Kastberg, "Cold atoms: A field enabled by light," *Europhys. Lett.* **110** (2015).
8. Y. Shevy and H. Deng, "Frequency-stable and ultranarrow-linewidth semiconductor laser locked directly to an atomic-cesium transition," *Opt. Lett.* **23**(6), 472–474 (1998).
9. H. Stoehr, E. Mensing, J. Helmcke, and U. Sterr, "Diode laser with 1 Hz linewidth," *Opt. Lett.* **31**(6), 736–738 (2006).
10. F. Schmid, J. Weitenberg, T. W. Hansch, T. Udem, and A. Ozawa, "Simple phase noise measurement scheme for cavity-stabilized laser systems," *Opt. Lett.* **44**(11), 2709–2712 (2019).
11. A. C. Wilson, J. C. Sharpe, C. R. McKenzie, P. J. Manson, and D. M. Warrington, "Narrow-linewidth master-oscillator power amplifier based on a semiconductor tapered amplifier," *Appl. Opt.* **37**(21), 4871–4875 (1998).
12. K. Bongs, Y. Singh, L. Smith, W. He, O. Kock, D. Swierad, J. Hughes, S. Schiller, S. Alighanbari, S. Origlia, S. Vogt, O. Sterr, C. Lisdat, R. Le Targat, J. Lodewyck, D. Holleville, B. Venon, S. Bize, G. P. Barwood, P. Gill, I. R. Hill, Y. B. Ovchinnikov, N. Poli, G. M. Tino, J. Stuhler, W. Kaenders, and S. Team, "Development of a strontium optical lattice clock for the SOC mission on the ISS," *C. R. Phys.* **16**(5), 553–564 (2015).
13. I. R. Hill, R. Hobson, W. Bowden, E. M. Bridge, S. Donnellan, E. A. Curtis, and P. Gill, "A low maintenance Sr optical lattice clock," *8th Symposium on Frequency Standards and Metrology 2015* 723 (2016).
14. S. A. Webster, M. Oxborrow, and P. Gill, "Subhertz-linewidth Nd : YAG laser," *Opt. Lett.* **29**(13), 1497–1499 (2004).
15. S. S. Sane, S. Bennetts, J. E. Debs, C. C. N. Kuhn, G. D. McDonald, P. A. Altin, J. D. Close, and N. P. Robins, "11 W narrow linewidth laser source at 780nm for laser cooling and manipulation of Rubidium," *Opt. Express* **20**(8), 8915–8919 (2012).

16. M. Guina, A. Rantamaki, and A. Harkonen, "Optically pumped VECSELs: review of technology and progress," *J. Phys. D: Appl. Phys.* **50**(38), 383001 (2017).
17. M. A. Holm, D. B. A. I. Ferguson, and M. D. Dawson, "Actively stabilized single-frequency vertical-external-cavity AlGaAs laser," *IEEE Photonics Technol. Lett.* **11**(12), 1551–1553 (1999).
18. A. Garnache, A. Laurain, M. Myara, J. P. Perez, L. Cerutti, A. Michon, G. Beaudoin, I. Sagnes, P. Cermak, and D. Romanini, "Design and properties of high-power highly-coherent single-frequency VECSEL emitting in the near- to mid-IR for photonic applications," *SPIE LASE - VECSELs I* 7919 (2011).
19. M. Y. A. Raja, S. R. J. Brueck, M. Osinski, C. F. Schaus, J. G. Mcinerney, T. M. Brennan, and B. E. Hammons, "Resonant Periodic Gain Surface-Emitting Semiconductor-Lasers," *IEEE J. Quantum Electron.* **25**(6), 1500–1512 (1989).
20. R. L. R. Celis and M. Martinelli, "Reducing the phase noise in diode lasers," *Opt. Lett.* **44**(13), 3394–3397 (2019).
21. S. Field, M. Finander, G. Niven, and W. Mackenzie, "Latest achievements of NECSEL visible extended cavity surface emitting lasers," *SPIE LASE - VECSELs V* 9349 (2015).
22. A. L. Schawlow and C. H. Townes, "Infrared and Optical Masers," *Phys. Rev.* **112**(6), 1940–1949 (1958).
23. C. H. Henry, "Theory of the Linewidth of Semiconductor-Lasers," *IEEE J. Quantum Electron.* **18**(2), 259–264 (1982).
24. S. D. Saliba and R. E. Scholten, "Linewidths below 100 kHz with external cavity diode lasers," *Appl. Opt.* **48**(36), 6961–6966 (2009).
25. B. Cocquelin, G. Lucas-Leclin, P. Georges, I. Sagnes, and A. Garnache, "Design of a low-threshold VECSEL emitting at 852 nm for Cesium atomic clocks," *Opt. Quantum Electron.* **40**(2-4), 167–173 (2008).
26. J. L. Hall, T. Baer, L. Hollberg, and H. G. Robinson, "Precision Spectroscopy and Laser Frequency Control Using FM Sideband Optical Heterodyne Techniques," in *Laser Spectroscopy V* 30 (Springer Berlin Heidelberg, 1981), 15–24.
27. R. W. P. Drever, J. L. Hall, F. V. Kowalski, J. Hough, G. M. Ford, A. J. Munley, and H. Ward, "Laser Phase and Frequency Stabilization Using an Optical-Resonator," *Appl. Phys. B* **31**(2), 97–105 (1983).
28. G. Di Domenico, S. Schilt, and P. Thomann, "Simple approach to the relation between laser frequency noise and laser line shape," *Appl. Opt.* **49**(25), 4801–4807 (2010).
29. K. R. Vogel, T. P. Dinneen, A. Gallagher, and J. L. Hall, "Narrow-line Doppler cooling of strontium to the recoil limit," *IEEE Trans. Instrum. Meas.* **48**(2), 618–621 (1999).
30. H. Katori, T. Ido, Y. Isoya, and M. Kuwata-Gonokami, "Magneto-Optical Trapping and Cooling of Strontium Atoms down to the Photon Recoil Temperature," *Phys. Rev. Lett.* **82**(6), 1116–1119 (1999).
31. T. Ido, T. H. Loftus, M. M. Boyd, A. D. Ludlow, K. W. Holman, and J. Ye, "Precision spectroscopy and density-dependent frequency shifts in ultracold Sr," *Phys. Rev. Lett.* **94** (2005).
32. J. E. Hastie, S. Calvez, M. D. Dawson, T. Leinonen, A. Laakso, J. Lyytikainen, and M. Pessa, "High power CW red VECSEL with linearly polarized TEM00 output beam," *Opt. Express* **13**(1), 77–81 (2005).
33. D. Paboeuf and J. E. Hastie, "Tunable narrow linewidth AlGaInP semiconductor disk laser for Sr atom cooling applications," *Appl. Opt.* **55**(19), 4980–4984 (2016).
34. E. Ponslet, "Piezo-Electric Actuator Initial Performance Tests," LIGO project report HYTEC-TN-LIGO **30**, 15p (1998).
35. E. D. Black, "An introduction to Pound-Drever-Hall laser frequency stabilization," *Am. J. Phys.* **69**(1), 79–87 (2001).
36. M. Tröbs and G. Heinzel, "Improved spectrum estimation from digitized time series on a logarithmic frequency axis," *Measurement* **39**(2), 120–129 (2006).
37. S. V. Kashanian, A. Eloy, W. Guerin, M. Lintz, M. Fouche, and R. Kaiser, "Noise spectroscopy with large clouds of cold atoms," *Phys. Rev. A*, 94 (2016).
38. N. Jornod, K. Gurel, V. J. Wittwer, P. Brochard, S. Hakobyan, S. Schilt, D. Waldburger, U. Keller, and T. Sudmeyer, "Carrier-envelope offset frequency stabilization of a gigahertz semiconductor disk laser," *Optica* **4**(12), 1482–1487 (2017).
39. M. Myara, M. Sellahi, A. Laurain, A. Michon, I. Sagnes, and A. Garnache, "Noise properties of NIR and MIR VECSELs," *SPIE LASE - VECSEL III* 8606 (2013).
40. G. M. Stéphan, T. T. Tam, S. Blin, P. Besnard, and M. Têtu, "Laser line shape and spectral density of frequency noise," *Phys. Rev. A* **71**(4), 043809 (2005).
41. P. H. Moriya and J. E. Hastie, "Sub-kHz linewidth VECSEL for cold atom experiments," in *Laser Congress 2018 (ASSL), OSA Technical Digest* (Optical Society of America, 2018), ATh5A.4.
42. P. Dumont, F. Camargo, J. M. Danet, D. Holleville, S. Guerandel, G. Pillet, G. Bailly, L. Morvan, D. Dolfi, I. Gozhyk, G. Beaudoin, I. Sagnes, P. Georges, and G. Lucas-Leclin, "Low-Noise Dual-Frequency Laser for Compact Cs Atomic Clocks," *J. Lightwave Technol.* **32**(20), 3817–3823 (2014).
43. S. C. Burd, D. T. C. Allcock, T. Leinonen, J. P. Penttinen, D. H. Slichter, R. Srinivas, A. C. Wilson, R. Jrdens, M. Guina, D. Leibfried, and D. J. Wineland, "VECSEL systems for the generation and manipulation of trapped magnesium ions," *Optica* **3**(12), 1294–1299 (2016).
44. E. C. Cook, P. J. Martin, T. L. Brown-Heft, J. C. Garman, and D. A. Steck, "High passive-stability diode-laser design for use in atomic-physics experiments," *Rev. Sci. Instrum.* **83**(4), 043101 (2012).
45. R. Schwarz, S. Dorscher, A. Al-Masoudi, S. Vogt, Y. Li, and C. Lisdat, "A compact and robust cooling laser system for an optical strontium lattice clock," *Rev. Sci. Instrum.* **90**(2), 023109 (2019).

46. D. Akamatsu, Y. Nakajima, H. Inaba, K. Hosaka, M. Yasuda, A. Onae, and F. L. Hong, "Narrow linewidth laser system realized by linewidth transfer using a fiber-based frequency comb for the magneto-optical trapping of strontium," *Opt. Express* **20**(14), 16010–16016 (2012).
47. O. I. Berdasov, A. Y. Gribov, G. S. Belotelov, V. G. Pal'chikov, S. A. Strelkin, K. Y. Khabarova, N. N. Kolachevsky, and S. N. Slyusarev, "Ultrastable laser system for spectroscopy of the S-1(0) - P-3(0) clock transition in Sr atoms," *Quantum Electron.* **47**(5), 400–405 (2017).
48. A. Smith, J. E. Hastie, H. D. Foreman, T. Leinonen, M. Guina, and M. D. Dawson, "GaN diode-pumping of red semiconductor disk laser," *Electron. Lett.* **44**(20), 1195–1196 (2008).
49. R. Casula, P. H. Moriya, G. A. Chappell, D. C. Parrotta, S. Ranta, H. Kahle, M. Guina, and J. E. Hastie, "GaN-diode-pumped AlGaInP VECSEL for strontium optical clocks," in *SPIE LASE - VECSELS IX*, (2019),
50. A. Ouvrard, A. Garnache, L. Cerutti, F. Genty, and D. Romanini, "Single-frequency tunable Sb-based VCSELS emitting at 2.3  $\mu\text{m}$ ," *IEEE Photonics Technol. Lett.* **17**(10), 2020–2022 (2005).
51. N. Poli, G. Ferrari, M. Prevedelli, F. Sorrentino, R. E. Drullinger, and G. M. Tino, "Laser sources for precision spectroscopy on atomic strontium," *Spectrochim. Acta, Part A* **63**(5), 981–986 (2006).
52. P. H. Moriya, "Data for: "Sub-kHz-linewidth VECSELS for cold atom experiments"," *University of Strathclyde* (2020). DOI: <https://10.15129/6a8ad2c5-9bec-41e7-bec4-38976ad1c590>.